DESY 96-223
hep-ph/9610489
October 1996

ISSN 0418-9833

arXiv:hep-ph/9610489v1 25 Oct 1996

# Inclusive Two–Jet Production in Photon–Photon Collisions: Direct and Resolved Contributions in Next–to–Leading Order QCD

T. Kleinwort*, G. Kramer
II. Institut für Theoretische Physik†
Universität Hamburg
D - 22761 Hamburg, Germany

**Abstract**

We have calculated inclusive two–jet production in photon–photon collisions superimposing direct, single–resolved and double–resolved cross sections for center–of–mass energies of TRISTAN and LEP1.5. All three contributions are calculated up to next–to–leading order. The results are compared with recent experimental data. Three NLO sets of parton distributions of the photon are tested.

*E–mail: tkleinw@ifh.de, present address: DESY–IfH Zeuthen, Platanenallee 6, 15735 Zeuthen

†Supported by Bundesministerium für Forschung und Technologie, Bonn, Germany under Contract 05 7HH92P(5) and EEC Program "Human Capital and Mobility" through Network "Physics at High Energy Colliders" under Contract CHRX–CT93–0357 (DG12 COMA)

# 1 Introduction

The production of high-$p_T$ jets probes the short-distance dynamics of photon-photon reactions. In addition to providing tests of perturbative QCD, $\gamma\gamma$ processes with real or almost real photons give us information on the photon structure function which is complementary to the information gained from deep inelastic scattering on a real photon. The latter process essentially probes the quark distribution while high-$p_T$ jet production is also sensitive to the gluon distribution of the photon.

As it is well known high-$p_T$ processes induced by real photons have a rather complex structure. This arises from the fact that the photon couples to the hard subprocess either directly or through its quark and gluon content.

In leading order QCD (LO) the cross section for the production of jets can therefore be decomposed into a direct, single-resolved, and double-resolved component. In next-to-leading order (NLO) the photon-quark collinear singularities in the direct and single resolved components are subtracted and absorbed into the quark distribution of the photon in accord with the factorization theorem. This subtraction at the factorization scale $M$ introduces an interdependence of the three components so that the separation into the direct, single-resolved, and double-resolved contributions becomes scale dependent. This means that in NLO all three components must be considered together and consistently be calculated up to NLO in the photon structure functions and in the hard scattering cross sections.

Complete NLO calculations have been done previously for the case of the inclusive single–jet cross section [1, 2, 3] and compared to experimental data from TRISTAN [4, 5]. Satisfactory agreement between data and theory has been found. In our previous work [2, 3] we also calculated the NLO inclusive two-jet cross sections for the direct and single-resolved contribution and estimated the double-resolved contribution by the LO calculation with $k$ factors taken from the NLO inclusive one-jet cross section. In the meantime the calculation of the NLO corrections for the double-resolved cross section has been completed also for the inclusive two-jet cross section using techniques also employed for the direct and single-resolved cross sections in our previous work [2, 3].

In this paper we shall present the complete NLO predictions for the inclusive two-jet cross section incorporating all three components, direct, single-resolved and double-resolved. We shall compare these predictions with the older TRISTAN data [4, 5] and with recent data from LEP at $e^+e^-$ energies of 130 and 136 $GeV$ (LEP1.5) [6]. The details of the NLO calculation of the double-resolved cross section are given elsewhere [7]. Those of the direct and single-resolved cross section are described in [3].

The outline of the rest of the paper is as follows. In section 2 we explain the formalism used to calculate the inclusive two-jet cross section. Section 3 contains our results for the cross sections and some studies on the overall scale dependence and the dependence of the two-jet cross section on the cone radius R. Here we also present the results for different sets of photon structure functions and the comparison with the TRISTAN and LEP1.5 data. Section 4 contains a short summary.

# 2 Inclusive Two-Jet Cross Sections

As explained in the introduction inclusive jet cross sections at large $p_T$ receive contributions from three parts according to how the incoming photons take part in the hard scattering subprocesses. For example, when both photons are resolved the inclusive two-jet cross section

has the following form

$$\frac{\mathrm{d}^3\sigma^{DR}}{\mathrm{d}p_T\mathrm{d}\eta_1\mathrm{d}\eta_2} = \sum_{i,j=q,g}\int\mathrm{d}x_1\int\mathrm{d}x_2\,F_{i/\gamma}(x_1,M)\,F_{j/\gamma}(x_2,M) \left(\left(\frac{\mathrm{d}^3\sigma^{DR}(ij\to\mathrm{jet}_1+\mathrm{jet}_2)}{\mathrm{d}p_T\mathrm{d}\eta_1\mathrm{d}\eta_2}\right)_{\mathrm{LO}}+\frac{\alpha_s(\mu)}{2\pi}K_{ij}^{DR}(R,M,\mu)\right) \quad (1)$$

In (1), $p_T$ is the transverse momentum of the measured or trigger jet with rapidity $\eta_1$. $\eta_2$ denotes the rapidity of another jet such that in the three-jet sample (in the NLO calculation only up to three jets occur in the final state, the photon remnant jets are not counted) these two jets have the largest and second largest $p_T$ ($p_{T1}, p_{T2} > p_{T3}$). The first term on the right-hand side of (1) stands for the LO cross section and the second term is the NLO correction which depends on the factorization scale $M$ at which the initial state singularities are absorbed into the parton distributions of the photon. $\mu$ is the renormalization scale. The variable $R$ is the usual cone size parameter which defines the size of the jets with transverse momentum $p_T$, rapidity $\eta$ and azimuthal angle $\phi$. When two partons fulfill the Snowmass constraint [8] with the cone size parameter $R$ they are recombined in one jet. The same jet definition is used in the analysis of the experimental data by the TOPAZ [4], AMY [5] and OPAL [6] collaborations. It is clear that either of the two jets can consist of a recombination of two partons inside a cone with radius $R$.

The NLO corrections in the hard scattering processes are calculated with the phase space slicing method using for the separation of the $\gamma\gamma \to 2$ jets and $\gamma\gamma \to 3$ jets cross sections an invariant mass cut-off $y$, defined as $2p_ip_j < ys$, where $s$ is the partonic center-of-mass energy squared. For example, the cross section for the direct process $\gamma\gamma \to q\bar{q}g$ has soft, initial, and final state collinear singularities. The $\gamma\gamma \to q\bar{q}g$ cross section is integrated over these singular regions up to the cut-off $y$ which isolates the respective singularities. These cancel against the singular contributions of the virtual corrections to $\gamma\gamma \to q\bar{q}$ and the subtraction terms at the scale $M$ to be absorbed into the parton distribution functions of the photon. Outside the cut-off region controlled by the parameter $y$ we have genuine $q\bar{q}g$ final states. In this contribution two of the partons are combined if they obey the Snowmass constraint. The LO contribution, the NLO virtual contributions, and the NLO corrections inside the $y$ cut contribute to the two-jet cross section together with the contributions inside the cone with radius $R$. The part of the $q\bar{q}g$ cross section not fulfilling the cone recombination condition is the 3-jet cross section from which we have calculated the inclusive 2-jet cross section as a function of $p_T$, $\eta_1$ and $\eta_2$.

For the exclusive 2-jet cross section $p_{T1} = p_{T2} = p_T$. To separate double singularities in the $q\bar{q}g$ contributions we have used the method of partial fractioning. The same partial fractioned expressions are applied for the calculation inside and outside the $y$ cut. Inside the $y$ cut the calculation is done analytically in the approximation that terms $O(y)$ are neglected. Outside the $y$ cut the contributions to the inclusive cross section are evaluated numerically with no further approximations. Because of the approximation in the analytic part, the parameter $y$ must be chosen very small, of the order of $10^{-3}$ to $10^{-4}$. For such values of $y$ the inclusive cross section should be independent of the invariant mass parameter $y$. However the inclusive two-jet cross section depends on the cone size $R$, which must be chosen as in the analysis of the experimental data. In the case of the single– and double–resolved contributions the calculation of the NLO corrections proceeds in the same way. For example, in the single–resolved case, we have in LO the contributions from $\gamma g \to q\bar{q}$ and $\gamma q \to qg$ and in NLO we must consider $\gamma g \to q\bar{q}g, \gamma q \to qq\bar{q}$ and $\gamma q \to qgg$ which are treated in the same fashion as the 3–parton contributions in the direct case. In the calculation of the double–resolved cross section we have no photons in the initial

state, only quarks and gluons, and we have many more channels to consider as processes with three partons in the final state, which will not be given here. Otherwise the calculation proceeds in a completely analogous way to the direct and single–resolved case.

Before the final results were obtained some tests of the NLO corrections have been performed. First we checked that the cross sections are independent of the cut-off $y$ if $y$ is chosen small enough. This was the case for $y \leq 10^{-3}$ in all considered cases. For $y > 10^{-3}$ we observed some small $y$ dependence which is caused by the approximation in the analytical part. Second the inclusive one–jet cross section for the double–resolved contribution was calculated and compared with our earlier results for which a completely different method for the cancellation of the infrared and collinear singularities was applied [2, 3]. Very good agreement was found in all channels. Third we tested that the sum of the NLO direct and the LO single–resolved cross section is independent of the factorization scale $M$. The same test was performed for the sum of the NLO single–resolved cross section and the LO double–resolved cross section. Details of these tests can be found in [7]. In this work also the details of the analytic calculation and the cancellation of the singularities for the NLO corrections of the double–resolved cross section are given. For the direct and the single–resolved cross sections the calculation of the NLO corrections was described earlier in [3] and [9], respectively, and also in [7].

For the calculation of the single– and double–resolved cross sections we need the parton distributions of the photon $F_{i/\gamma}$ which appear in (1) and in the equivalent formula for the single-resolved cross section (see [2]). We have chosen the NLO set of Glück, Reya and Vogt (GRV) in the $\overline{\rm MS}$ scheme [10] as our standard set. For a comparison we shall employ also the $\overline{\rm MS}$ sets of Gordon and Storrow [11] and of Aurenche et al. [12]. We choose all scales $\mu = M = p_T$ except when we test the scale dependence. $\alpha_s$ is calculated from the two–loop formula with $N_f = 4\,(5)$ massless flavours with $\Lambda^{(4)}_{\overline{\rm MS}} = 0.20\,GeV (\Lambda^{(5)}_{\overline{\rm MS}} = 0.13\,GeV)$ for the $e^+e^-$ center of mass energy $\sqrt{S} = 58\,GeV (\sqrt{S} = 133\,GeV)$. The charm, respectively, bottom quarks are also treated as light flavours with the boundary condition that the charm (bottom) content of the photon structure function vanishes for $M^2 < m_c^2\,(m_b^2)$ with $m_c = 1.5\,GeV (m_b = 5.0\,GeV)$ for the GRV parton distributions [10]. For the other two sets the treatment of heavy flavours is somewhat different. The details are found in the respective references [11, 12].

# 3 Results and Comparison with Data from TOPAZ, AMY, and OPAL

In $e^+e^-$ collisions the jets are produced via the exchange of two almost real photons. The spectrum of these small $Q^2$ photons is described by the Weizsäcker-Williams approximation [13]

$$F_{\gamma/e}(z,E) = \frac{\alpha}{2\pi}\frac{1+(1-z)^2}{z}\left\{\ln\left(\frac{E^2\theta^2_{\rm max}(1-z)^2 + m_e^2 z}{m_e^2 z^2}\right) + 2(1-z)\left(\frac{m_e^2 z}{E^2\theta^2_{\rm max}(1-z)^2 + m_e^2 z^2} - \frac{1}{2}\right)\right\} \qquad (2)$$

where $\theta_{\rm max}$ is the maximally allowed angle of the electron (positron) which is given experimentally by the anti-tagging counters. $E$ is the beam energy of the electron (positron) and $z = E_\gamma/E$ is the fraction of the electron (positron) energy transferred to the respective photon.

Then the inclusive two-jet cross section for the reaction $e^+ + e^- \to e^+ + e^- + {\rm jet}_1 + {\rm jet}_2 + X$

is calculated from

$$\frac{\mathrm{d}^3\sigma(e^+ + e^- \to e^+ + e^- + \mathrm{jet}_1 + \mathrm{jet}_2 + X)}{\mathrm{d}p_T \mathrm{d}\eta_1 \mathrm{d}\eta_2} = \int \mathrm{d}z_1 \int \mathrm{d}z_2 \, F_{\gamma/e}(z_1, E) \, F_{\gamma/e}(z_2, E) \frac{\mathrm{d}^3\sigma(\gamma + \gamma \to \mathrm{jet}_1 + \mathrm{jet}_2 + X)}{\mathrm{d}p_T \mathrm{d}\eta_1 \mathrm{d}\eta_2} \qquad (3)$$

where the cross section on the right-hand side is for the interaction of two real photons ($Q^2 = 0$) and is obtained from (1) for the double-resolved case and similar formulas for the direct and single-resolved $\gamma\gamma$ cross section (see [2]).

First we show in Fig. 1 the dependence of the inclusive 2–jet cross section on the cone radius $R$ for the special case of LEP2 kinematics, $\sqrt{S} = 175\,GeV, \theta_{\max} = 1.72°$, since we cannot expect this dependence to be tested with TRISTAN or LEP1.5 data. Of course, the LO cross section is independent of $R$ which is shown as the broken line in Fig. 1. In the NLO calculation the cross section increases with increasing $R$, first almost linearly in $\ln R$ for $R$ values up to 0.75 and somewhat stronger for $R > 0.75$. At $R \simeq 0.9$ the LO and NLO cross sections are equal for the special kinematical point $p_T = 10\,GeV, \eta_1 = \eta_2 = 0$. Therefore for $R$ values, chosen between 0.7 and 1.0, the higher order corrections are moderate. The LO curve is obtained with the two-loop formula with the same $\Lambda_{\overline{\mathrm{MS}}}$ value and with the same NLO photon structure functions from GRV. In a genuine LO calculation with one–loop $\alpha_s$ and LO structure functions the cross section is somewhat larger. That the NLO corrections near $R = 1$ are not very large is due to the dominance of the direct contribution which is not changed by the NLO corrections very much [2, 3] in contrast to the NLO corrections for the double–resolved cross section [7].

In Fig. 2, 3, and 4 the inclusive two-jet cross sections $\frac{\mathrm{d}^3\sigma}{\mathrm{d}p_T \mathrm{d}\eta_1 \mathrm{d}\eta_2}$ are plotted as a functions of $p_T$, integrated over the rapidities $\eta_1$ and $\eta_2$ as in the experimental analysis of the TOPAZ [4], AMY [5] and OPAL [6] collaborations. The conditions for the TOPAZ experiment are $\theta_{\max} = 3.2°, z_1, z_2 \leq 0.75$ and $|\eta_1|, |\eta_2| \leq 0.7$. The cone radius $R = 1$ is used in all three figures. The comparison with the TOPAZ data [4] is seen in Fig. 2. The full curve is the sum of the direct, single–resolved and double–resolved contributions. The separate cross sections are also plotted. From these curves one can see that at the TRISTAN energy the resolved part is significant only at very small $p_T$. At large $p_T \simeq 8\,GeV$ the direct contribution is dominant. But both, the double–resolved and even more the single–resolved cross section make a non–negligible contribution. The agreement of the theoretical prediction with the TOPAZ data is very good. It is clear from this comparison that the data cannot be explained by the direct contribution alone even at the larger $p_T$. In Fig. 3 the same curves for the AMY experiment are shown. In this experiment the cuts are $\theta_{\max} = 13°$ and $|\eta_1|, |\eta_2| \leq 1$. $z_1$ and $z_2$ are not restricted further. We show again the three contributions, the direct, single–resolved and double–resolved cross section. The data points must be compared with the full curve. The agreement with the theoretical curve is again quite good. The AMY cross section is larger than the TOPAZ cross section, essentially since $\theta_{\max}$ is larger. In the fall of 1995 LEP was run at center-of-mass energies of 130 and $136\,GeV$. During this rather short run the OPAL collaboration was able to measure inclusive jet cross sections and analyze them with the cone jet finding algorithm [6]. The cone radius was also $R = 1$. In Fig. 4 we show their data of the inclusive two-jet cross section together with our prediction (full curve) and the cross sections for the direct, single–resolved and double–resolved part. The kinematical constraints are $\theta_{\max} = 1.43°, |\eta_1|, |\eta_2| \leq 1$. Because of the larger c.m. energy we have taken $N_f = 5$ and the corresponding $\Lambda_{\overline{\mathrm{MS}}} = 0.130\,GeV$. At small $p_T$ the data are very accurate. The combined statistical and systematic errors are shown. The agreement of the theory with the data is good

over the whole $p_T$ range. We see that the double–resolved contribution is much more important at this higher energy. It gives the dominant contribution for $p_T \leq 5\,GeV$. Even at $p_T = 16\,GeV$ the direct contribution is only 60% of the total. Except for the last high $p_T$ point which has a larger error the pure direct curve is not consistent with the data. This shows that the other two contributions, the single–resolved and double–resolved, are needed to explain the data. The OPAL collaboration measured also the inclusive single–jet cross section. The comparison of their data with our predictions is shown in [6] and [7]. The agreement between theory and the data is as good as in the two-jet case. The inclusive two-jet cross section for LEP1.5 contains an extra factor 2 as compared to the definition used for the TRISTAN energy in order to account for the definition as used in [6].

In all the comparisons between experiment and theory shown above, we employed the GRV presentation of the parton distributions of the photon. Other NLO parton distributions are those of Gordon and Storrow [11] and Aurenche et al. [12]. Before we compare the data with predictions based on these other parton distributions we investigate the scale dependence of the inclusive two-jet cross sections for the two $e^+e^-$ c.m. energies corresponding to TRISTAN and LEP1.5. The results are shown in Fig. 5a,b where we have plotted the two-jet cross sections for three different scales $\mu = M = \xi p_T$ with $\xi = 1/2$, 1 and 2, and compared them with the TOPAZ (Fig. 5a) and OPAL data (Fig. 5b). In both cases the cross section is remarkably independent of the scale change. Only at rather small $p_T < 4\,GeV$ the cross section in Fig. 5a exhibits some scale change. For $p_T > 4\,GeV$ the cross section at $\sqrt{S} = 58\,GeV$ deviates less than $\pm 4\%$ from the standard with $\xi = 1$. Similarly the cross section at $\sqrt{S} = 133\,GeV$ shown in Fig. 5b varies by less than $\pm 2\%$ above $p_T = 8\,GeV$. This small scale change of the $\gamma\gamma$ jet cross sections (the inclusive one–jet cross section shows a similar behaviour) results from the fact that the scale change originating from the change of the renormalization scale $\mu$ leading to a decrease of the cross section with increasing $\xi$ is to a large extend cancelled by the dependence on the factorization scale $M$, which is opposite to the change in $\mu$. The dependence on $M$ is mostly cancelled between the NLO direct and the LO single-resolved cross section and similarly between NLO single-resolved and LO double-resolved cross section [7]. But some dependence on $M$ remains when all three cross sections are evaluated in NLO. Thus this reduced scale dependence of the $\gamma\gamma$ jet cross sections would be a good place to determine $\Lambda_{\overline{\rm MS}}$. For this we need photon structure functions with varying $\Lambda_{\overline{\rm MS}}$ which are not available yet and accurate data in particular for large $p_T$. In order to see the change of the two–jet cross section when we change from $\Lambda^{(5)}_{\overline{\rm MS}} = 0.130\,GeV$ to $\Lambda^{(5)}_{\overline{\rm MS}} = 0.250\,GeV$ in the formula for $\alpha_s$ we have plotted the cross section for this large value of $\Lambda_{\overline{\rm MS}}$ also in Fig. 5b. As to be expected the cross section is larger now. At the smaller $p_T < 5\,GeV$ the data points lie below the theoretical curve. Since $\Lambda_{\overline{\rm MS}}$ was not changed in the photon structure function consistently we do not draw any conclusions from this observation. At large $p_T$ the data points are still consistent with the theoretical curve for the larger $\Lambda^{(5)}_{\overline{\rm MS}}$. The equivalent result at $\sqrt{S} = 58\,GeV$ is shown in Fig. 5a, where we compare the results for $\Lambda^{(4)}_{\overline{\rm MS}} = 0.200\,GeV$ with $\Lambda^{(4)}_{\overline{\rm MS}} = 0.358\,GeV$ which is equivalent to $\Lambda^{(5)}_{\overline{\rm MS}} = 0.250\,GeV$ when we choose four active flavours. Due to the larger experimental errors the curve with the larger $\Lambda_{\overline{\rm MS}}$ value is still compatible with the data. At the larger $p_T$ the agreement is even somewhat improved. This shows that with the limited experimental accuracy of the data at both energies it seems difficult to draw clear conclusions even if the photon structure functions were given for varying $\Lambda_{\overline{\rm MS}}$.

In Fig. 6a,b we investigated the influence of the gluon distribution of the photon on the two–jet cross section. It is clear that the gluon distribution will have a remarkable influence only at small $p_T$ since this distribution function is dominant for small $x$. To see this we have assumed

$F_{g/\gamma} = 0$ with the assumption that the quark distribution functions are already well enough constrained by the deep inelastic $e$–$\gamma$ scattering data. As is seen in Fig. 6a,b the prediction with $F_{g/\gamma} = 0$ gives very bad agreement with the data at small $p_T$ ($p_T < 5\,GeV$ in Fig. 6a and $p_T < 8\,GeV$ in Fig. 6b). From this we conclude that the two-jet data require a non-vanishing $F_{g/\gamma}$ in the photon structure function. This agrees with earlier findings in [4, 5] on the basis of more model dependent calculations and with LO calculations in [14] based on new GS structure functions.

The last point is the prediction for other parton distributions of the photon than the GRV distribution in NLO. The comparison is shown in Fig. 7a,b together with the TOPAZ and OPAL experimental data. As we can see there is little difference between the results for the GRV [10] and the ACFGP [12] structure functions. The cross sections for the GS [11] distribution functions are somewhat smaller than for GRV. In average, for both c.m. energies, the data agree better with the GRV and ACFGP curve than with the curve based on the GS structure function, in particular in the comparison with the TOPAZ data. In order to exclude one of these structure functions much more accurate data are needed. In general, we conclude, that all three NLO parton distributions of the photon account remarkably well for the existing data of the inclusive two-jet production. It is clear, that additional information, as for example, the rapidity distributions for the two jets could constrain these structure functions further.

The same comparison has been done with the AMY two-jet data. Since in this case, the GRV curve lies at small $p_T$ above the data points the agreement with the prediction with the GS structure function is better than for the TOPAZ data.

Overall we can state that the agreement between the theoretical predictions and the measurements of the two–jet cross sections is remarkably good. This is true for the magnitude of the cross section and its shape as a function of $p_T$. We should not conceal, however, that the NLO calculation gives the jet cross sections for massless partons, whereas the experimental jet cross sections are measured from hadrons. Assuming the usual parton–hadron duality, no difference between parton and hadron level would be observed. This parton–hadron duality is very well obeyed in jet production for $e^+e^-$ annihilation at the $Z$ resonance. In this case the hard scale is larger than in the $\gamma\gamma$ processes, so that it is problematic to draw any firm conclusions from it. On the other hand it is not easy to estimate the hadronization effects for jet production in $\gamma\gamma$ processes. For this one needs a Monte Carlo routine which generates the final state partons including the NLO correction with subsequent fragmentation into hadron jets. Such a routine is not available yet. Estimates on the basis of LO Monte Carlos may not be too conclusive. Further details for this case are reported in [6].

# 4 Summary

Differential inclusive two–jet cross sections $\mathrm{d}\sigma/\mathrm{d}p_T$ have been calculated as a function of $p_T$ in NLO for the direct, single–resolved and double–resolved contributions. The superposition of these cross sections are compared to the TOPAZ, AMY and OPAL data. We obtained good agreement between measured data and the theoretical predictions. The same is true for the single inclusive cross sections [6, 7]. The single– and double–resolved cross sections are obtained with the GRV [10] photon structure function. Two other sets GS [11] and ACFGP [12] were also investigated. With them the data are described almost equally well. The $\gamma\gamma$ jet cross sections are remarkably stable against scale changes. With increasing center–of–mass energy the double–resolved contribution becomes more and more important. This is clearly seen by comparing the prediction for the TRISTAN and LEP1.5 energies. Similar to earlier findings

we exclude a description of the data without a gluon distribution in the photon. It is hoped that more accurate data from LEP2 may be able to constrain the parton distributions of the photon further.

# 5 Acknowledgements

We thank S. Söldner–Rembold for information about the OPAL measurements and for communicating the data before publication. We are grateful to M. Klasen for reading the manuscript.

# References

[1] P. Aurenche, J.–Ph. Guillet, M. Fontannaz, Y. Shimizu, J. Fujimoto, K. Kato, Progr. Theoret. Phys. 92 (1994) 175.

[2] T. Kleinwort, G. Kramer, Phys. Lett. B370 (1996) 141.

[3] T. Kleinwort, G. Kramer, Nucl. Phys. B477 (1996) 3.

[4] H. Hayashi et al., TOPAZ Collaboration, Phys. Lett. B314 (1993) 149.

[5] B.J. Kim et al., AMY Collaboration, Phys. Lett. B325 (1994) 248.

[6] K. Ackerstaff et al., OPAL Collaboration, CERN-PPE/96-132, September 1996, submitted to Z. Phys. C.

[7] T. Kleinwort, doctoral thesis, University of Hamburg, September 1996, DESY 96-195; M. Klasen, T. Kleinwort, G. Kramer, in preparation.

[8] J.E. Huth et al., Proc. of the 1990 DPF Summer Study on High Energy Physics, Snowmass, Colorado, edited by E.L. Berger, World Scientific, Singapore, 1992, p. 134.

[9] M. Klasen, G. Kramer, Z. Phys. C72 (1996) 107.

[10] M. Glück, E. Reya, A. Vogt, Phys. Rev. D46 (1992) 1973.

[11] L.E. Gordon, J.K. Storrow, Z. Phys. C56 (1992) 307.

[12] P. Aurenche, P. Chiapetta, M. Fontannaz, J.-Ph. Guillet, E. Pilon, Z. Phys. C56 (1992) 589.

[13] S. Frixione, M.L. Mangano, P. Nason, G. Ridolfi, Phys. Lett. B319 (1993) 339. For a review of photon fluxes in the equivalent photon approximation see P. Kessler, Proc. of the Workshop on Two-Photon Physics at LEP and HERA, Lund, Eds. G. Jarlskog and L. Jönsson, Lund University, 1994, p. 183.

[14] L.E. Gordon, J.K. Storrow, preprint ANL-HEP-PR-96-33, MC-TH-96-16.

# 6 Figure Captions

**Fig. 1:** The inclusive two–jet cross section as a function of the cone radius $R$ for LEP2 kinematics and $p_T = 10\,GeV, \eta_1 = \eta_2 = 0$.

**Fig. 2:** Inclusive two–jet cross section $\mathrm{d}\sigma/\mathrm{d}p_T$ with $R = 1$ as a function of $p_T$ for direct (dashed), single–resolved (dashed–dotted) and double–resolved (dotted) production in NLO. The full curve is the sum of all three components compared to TOPAZ data ($|\eta_1|, |\eta_2| < 0.7$)

**Fig. 3:** Inclusive two–jet cross section $\mathrm{d}\sigma/\mathrm{d}p_T$ with $R = 1$ as a function of $p_T$ for direct (dashed), single–resolved (dashed–dotted) and double–resolved (dotted) production in NLO. The full curve is the sum of all three components compared to AMY data ($|\eta_1|, |\eta_2| < 1$)

**Fig. 4:** Inclusive two–jet cross section $\mathrm{d}\sigma/\mathrm{d}p_T$ with $R = 1$ as a function of $p_T$ for direct (dashed), single–resolved (dashed–dotted) and double–resolved (dotted) production in NLO. The full curve is the sum of all three components compared to OPAL data ($|\eta_1|, |\eta_2| < 1$).

**Fig. 5:** Inclusive two–jet cross sections $\mathrm{d}\sigma/\mathrm{d}p_T$ for three different scales $\mu = M = \xi p_T$ with $\xi = \frac{1}{2}$ (dashed), $\xi = 1$ (full), $\xi = 2$ (dotted) and different $\Lambda_{\overline{\mathrm{MS}}}$ (dashed–dotted) compared to (a) TOPAZ data ($\Lambda^{(4)}_{\overline{\mathrm{MS}}} = 0.358\,GeV$) and (b) OPAL data ($\Lambda^{(5)}_{\overline{\mathrm{MS}}} = 0.250\,GeV$).

**Fig. 6:** Inclusive two–jet cross section $\mathrm{d}\sigma/\mathrm{d}p_T$ with GRV parton distributions and with $F_{g/\gamma} = 0$ (dashed) and $F_{g/\gamma} \neq 0$ (full) compared to (a) TOPAZ data and (b) OPAL data.

**Fig. 7:** Inclusive two–jet cross section $\mathrm{d}\sigma/\mathrm{d}p_T$ for different parton distribution sets: GRV [10] (full), GS [11] (dashed) and ACFGP [12] (dotted) compared to (a) TOPAZ and (b) OPAL two-jet data.

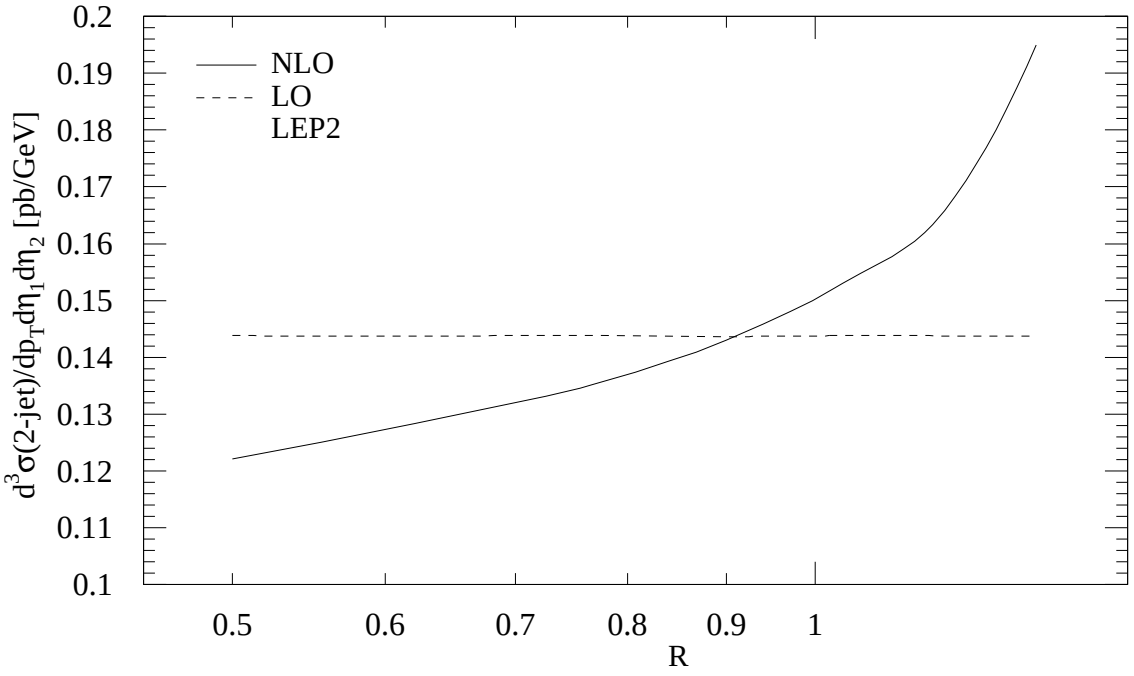



Figure 1:

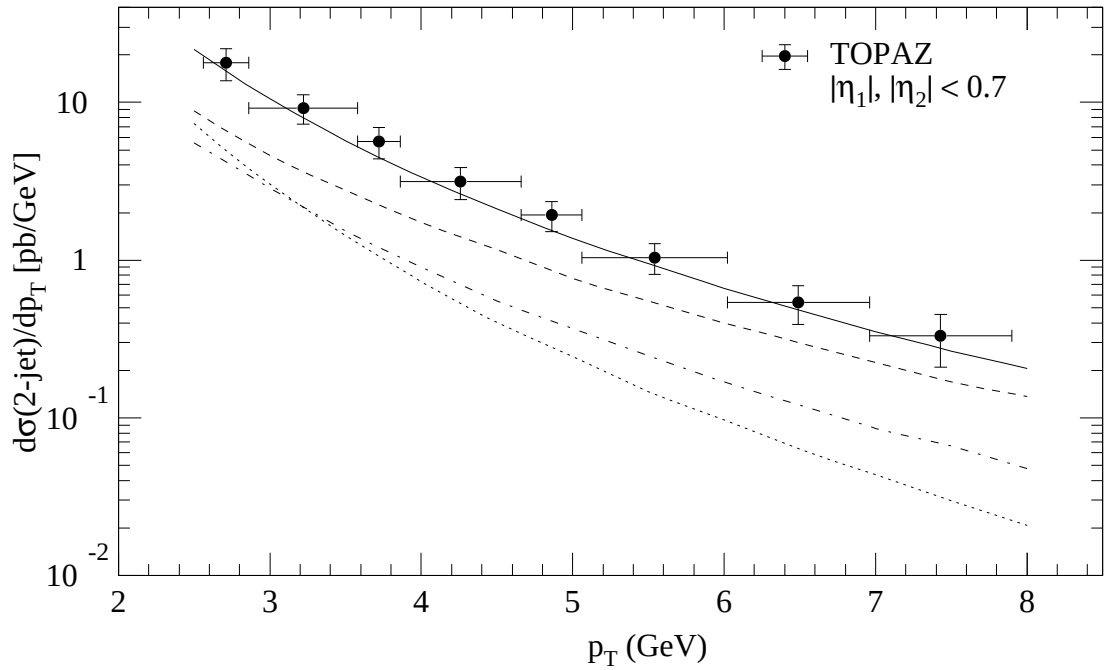



Figure 2:

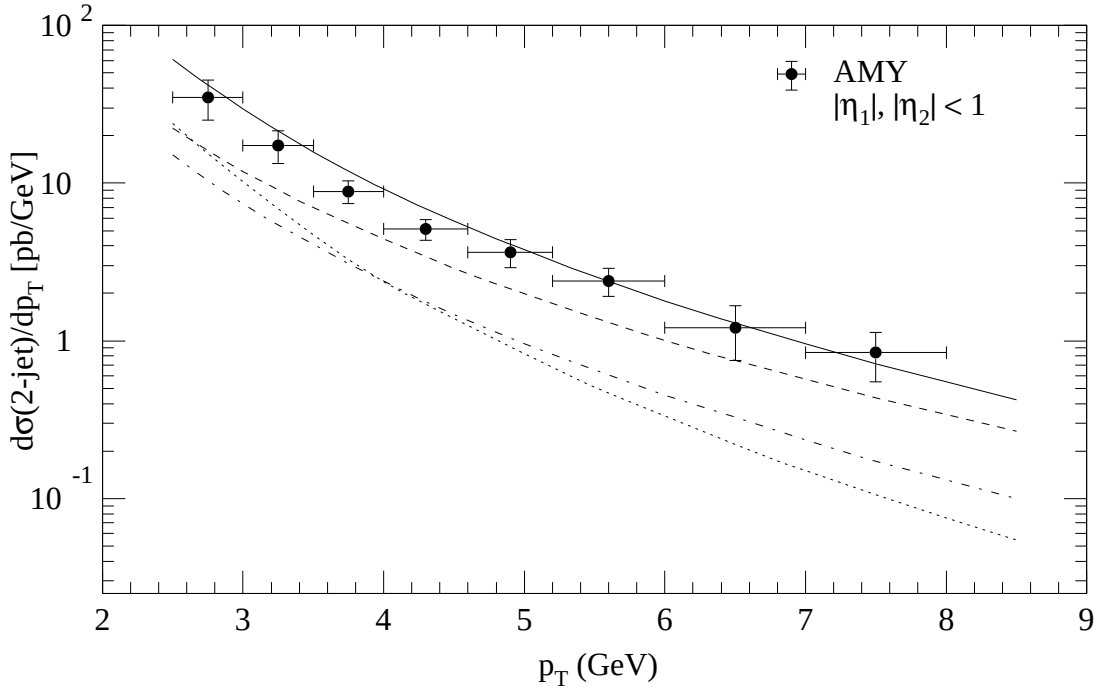



Figure 3:

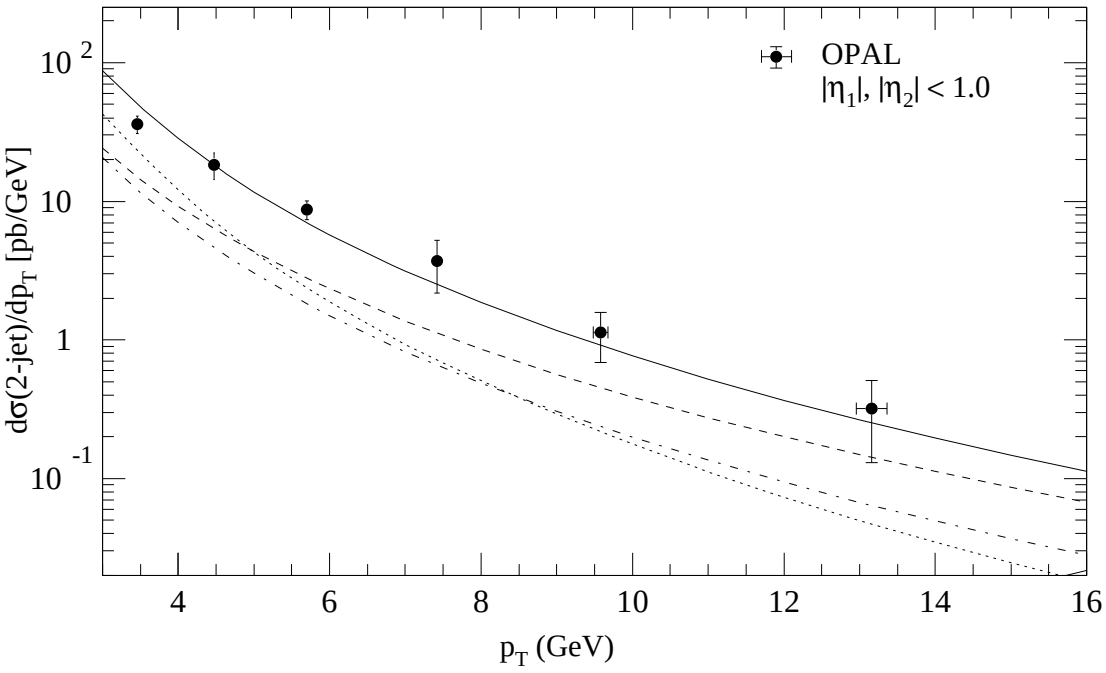



Figure 4:

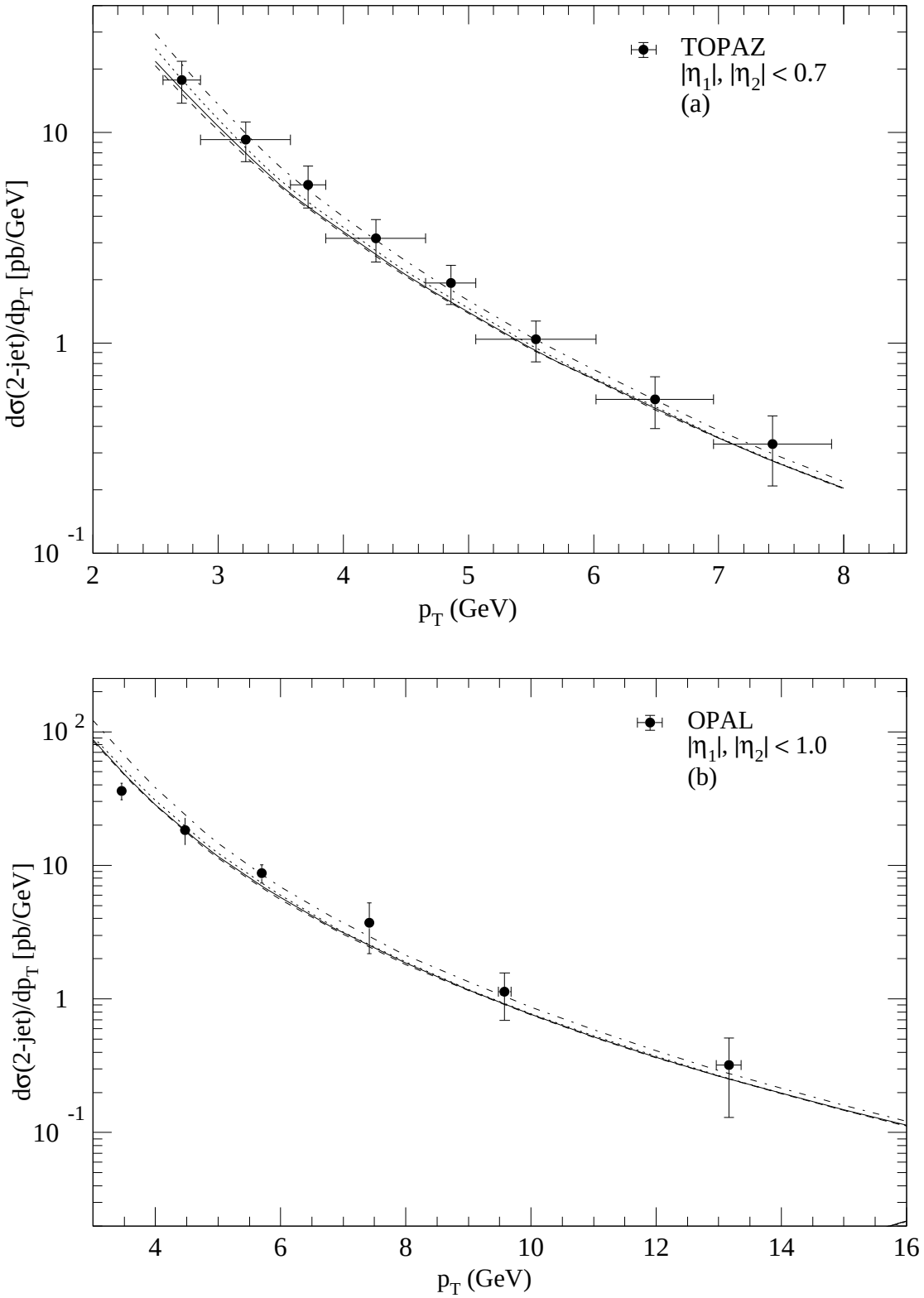

TOPAZ
|η1|, |η2| < 0.7
(a)
dσ(2-jet)/dpT [pb/GeV]
pT (GeV)
OPAL
|η1|, |η2| < 1.0
(b)
dσ(2-jet)/dpT [pb/GeV]
pT (GeV)

Figure 5:

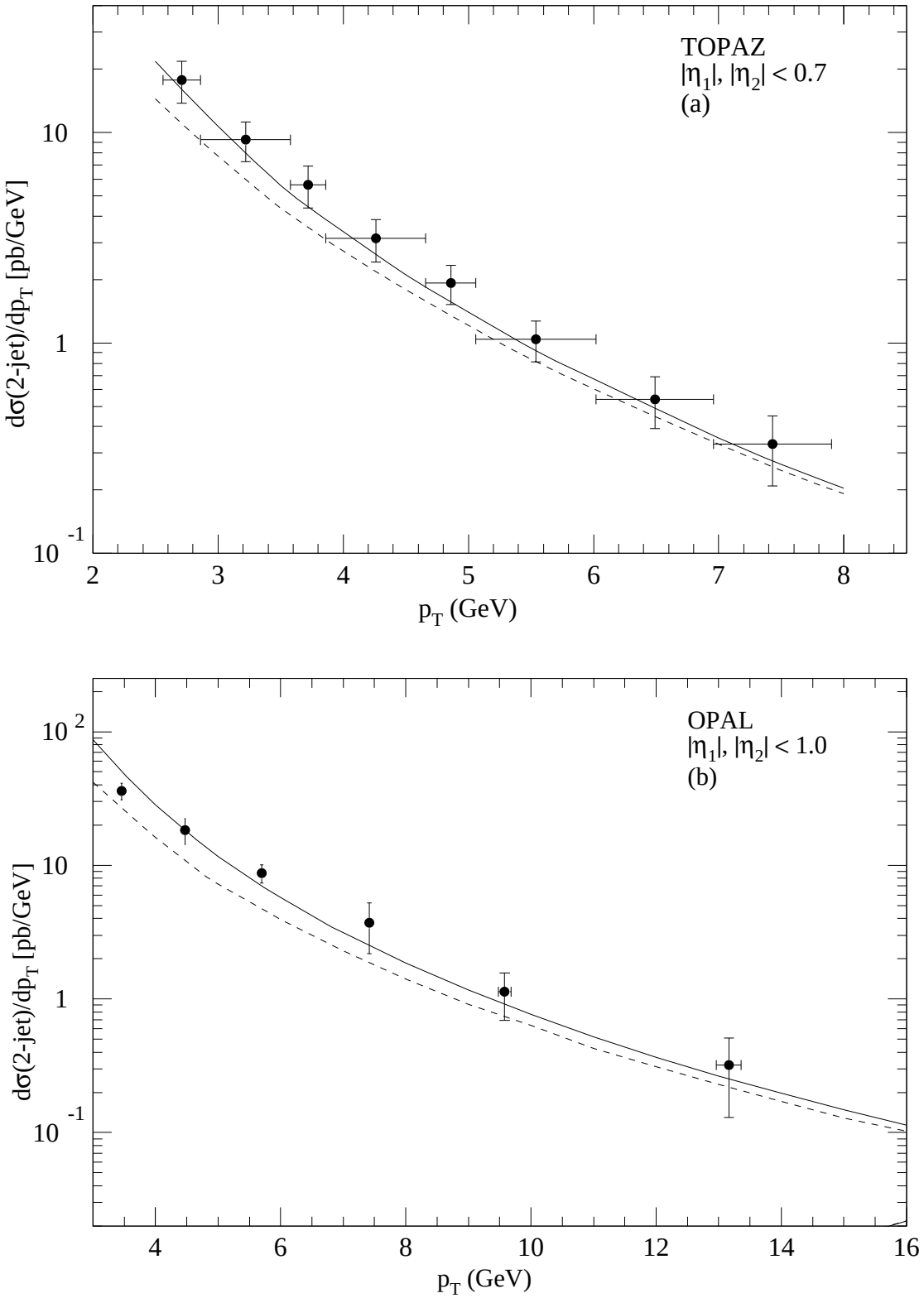

TOPAZ
$|\eta_1|, |\eta_2| < 0.7$
(a)
$d\sigma(2\text{-jet})/dp_T$ [pb/GeV]
$p_T$ (GeV)
OPAL
$|\eta_1|, |\eta_2| < 1.0$
(b)
$d\sigma(2\text{-jet})/dp_T$ [pb/GeV]
$p_T$ (GeV)

Figure 6:

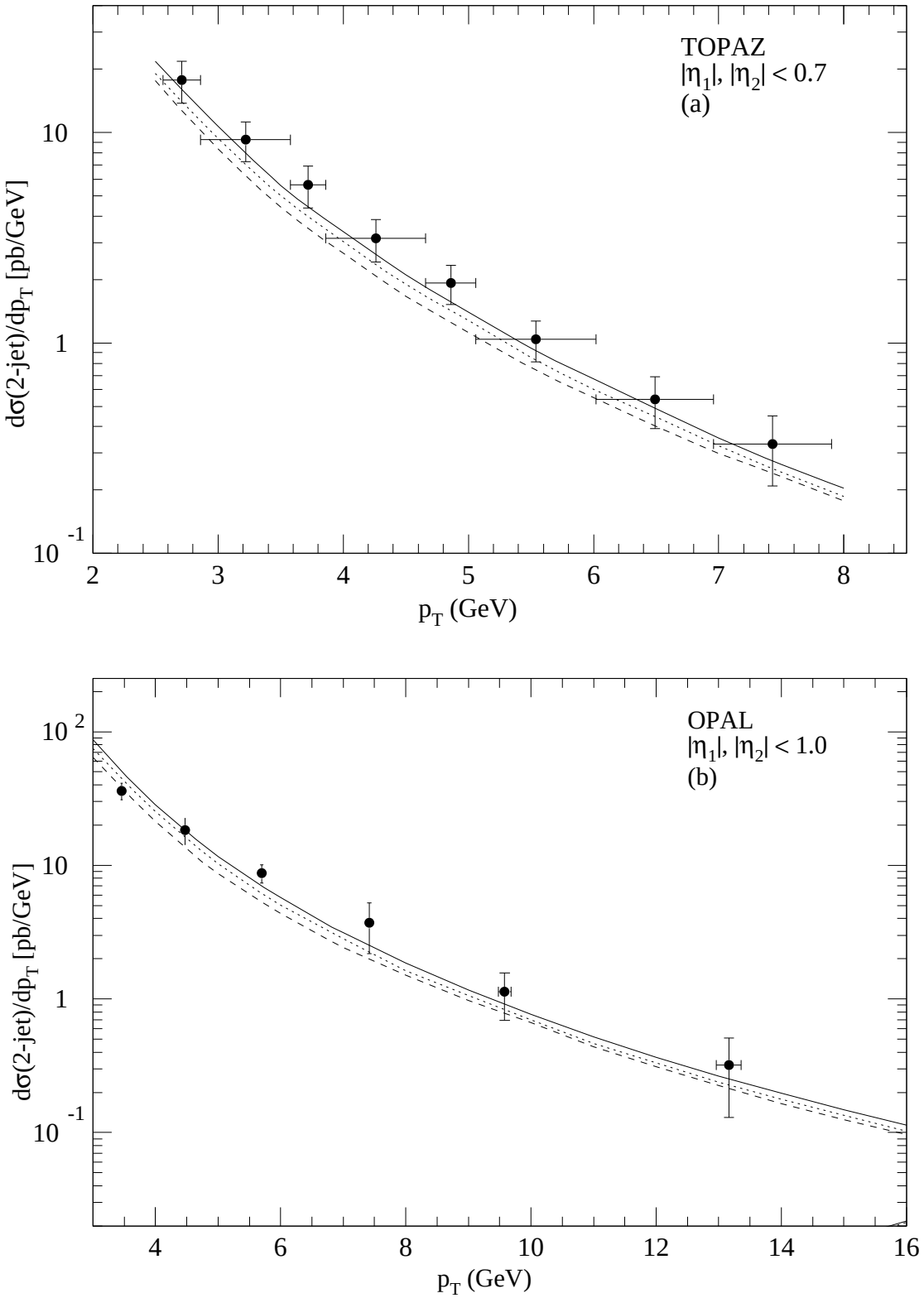

TOPAZ
$|\eta_1|, |\eta_2| < 0.7$
(a)
$d\sigma(2\text{-jet})/dp_T$ [pb/GeV]
$p_T$ (GeV)
OPAL
$|\eta_1|, |\eta_2| < 1.0$
(b)
$d\sigma(2\text{-jet})/dp_T$ [pb/GeV]
$p_T$ (GeV)

Figure 7: